CHARACTERISTICS OF PHENOL-FORMALDEHYDE ADHESIVE BONDS IN STEAM INJECTION PRESSED FLAKEBOARD

Stephen E. Johnson

Coatings Formulation Chemist
Akzo Coatings Inc.
P.O. Box 4627
2837 Roanoke Ave., S.W.
Roanoke, VA 24015

and

Frederick A. Kamke

Associate Professor
Virginia Tech
Department of Wood Science and Forest Products
Brooks Forest Products Center
1650 Ramble Road
Blacksburg, VA 24061

(Received July 1992)

ABSTRACT

A better understanding of the mechanisms involved in phenol-formaldehyde resin-wood bonding is needed to design adhesive systems that can adequately develop bond strength in a humid environment. This study was performed to determine how the molecular weight distribution of a liquid resole phenol-formaldehyde adhesive affects mechanical properties and adhesive flow in flakeboard bonded during steam injection pressing. The performance of three adhesives, differing only in molecular weight distribution, was studied. For all adhesives, mechanical properties of specimens located on the edge of the panel were found to be superior to those located in the center of the board. Excessive moisture present in the center of the mat was believed to be responsible for poor bonding. Edge internal bond strength improved with higher weight average molecular weight adhesive. Fluorescence microscopy and image analysis techniques were used to measure flow of adhesive into the wood substrate before and after exposure to a steam injection pressing environment. Flakes wetted with adhesive and not exposed to a pressing environment had more adhesive penetration with the lowest weight average molecular weight adhesive. Deeper and less concentrated adhesive penetration was measured in flakes exposed to a steam injection environment, with a smaller apparent difference between the three adhesives.

Keywords: Phenol-formaldehyde, steam injection pressing, fluorescence microscopy, image analysis, wood bonding.

INTRODUCTION

Recent commercial applications of steam injection pressing have renewed interest in this pressing technique. Steam injection during pressing rapidly transfers heat throughout the wood particulate mat, facilitating faster cure of thermosetting adhesives. Thus, steam injection pressing has the advantage of reduced press times as compared to conventional hot pressing, allowing production of thicker wood products. The injection of saturated steam into a mat creates a host of steam-related pressing variables, as well as introducing an adhesive curing environment that is different from the mat environment that exists during conventional hot pressing. During steaming, some steam condenses, thus releasing the heat of condensation in the mat. However, conden-

Wood and Fiber Science, 26(2), 1994, pp. 259–269

sation creates a humid environment and perhaps a substantial quantity of liquid water, which is not desirable for curing condensation polymers such as urea-formaldehyde and phenol-formaldehyde resins. Steam injection environments are believed to affect phenol-formaldehyde (PF) adhesive bonding in at least two areas: (1) moisture-induced effects on condensation polymerization kinetics, and (2) excessive flow of the adhesive from the bondline during and after steaming due to its solubility in water.

The objectives of this project were to determine how the mechanical properties and adhesive flow in flakeboard panels produced with steam injection pressing were affected by the molecular weight distribution of a liquid resole PF. Fluorescence microscopy and image analysis techniques were used to quantify flow of the adhesive into unpressed wood flakes and flakes exposed to a severe steam injection pressing environment.

BACKGROUND

The responses of a steam injection mat environment to adjustment of steam time, steam pressure, board thickness, adhesive type, and mat density range during the injection of steam have been measured (Geimer et al. 1991; Hata et al. 1989). Saturated steam conditions prevail through most of a steam injection pressing cycle, except for a brief period following the injection of steam and prior to venting the press manifold to atmosphere (Geimer et al. 1991). During the period immediately following steam injection, vapor pressure measurements indicate that significant condensation may occur in the mat. Acceptable board properties can be formed in that type of mat environment with a liquid resole PF by using high temperatures with a long steaming schedule.

Efforts have been made to simulate steam injection bonding conditions and monitor thermoset adhesive cure (Geimer and Christiansen 1991). A high humidity environment (91% RH) could accelerate development of adhesive stiffness and degree of chemical cure of a non-aqueous PF as judged by dynamic mechanical analysis (DMA) and differential scanning calorimetry (DSC), respectively. Moisture-induced plasticization of the adhesive in a humid environment may increase polymer chain mobility and facilitate crosslinking. However, with lap shear specimens prepared using aqueous PF at 115 C, bond strength development was greatest when bonds were formed in an intermediate relative humidity (41%), while bonds that were formed in the highest humidity (91%) were the weakest. Measured hardness of an aqueous PF adhesive cured in a steam environment in which temperatures ranged from 120 C to 200 C showed that the PF adhesive required long steam times and high temperatures to cure, and the adhesive had less than 20% of the hardness of a PF adhesive fully cured in a 160 C oil bath (Subiyanto et al. 1989).

Mechanical properties of panels and adhesive flow characteristics have been shown to be affected by the molecular weight distribution of liquid resole PF adhesives used in conventional hot-pressing. Laminated veneer lumber (LVL) loaded to failure after accelerated aging tests has indicated that higher wood failure can be obtained with neat PF resins that have low weight average molecular weight (Gollob et al. 1985). Poor neat adhesive performance has been obtained with a high weight average molecular weight adhesive with a large degree of molecular branching. When extenders and additives are used with the adhesive, the effects of individual variables are masked in a complex interrelationship (Gollob et al. 1985). Low molecular weight adhesive fractions may penetrate wood cell walls in veneers and serve as a primer by facilitating adsorption of higher molecular weight fractions (Nearn 1974).

The weight average molecular weight of PF adhesives used in veneered panels is several orders of magnitude larger than in PF adhesives used with nonveneered panels. Internal bond strength has been shown to increase using

larger proportions of high molecular weight fractions of PF adhesive during conventional hot-pressing of oak flakeboard. Low and medium molecular weight fractions are hypothesized to over-penetrate the wood substrate, thus "starving" the bondline (Wilson et al. 1979). Low molecular weight fractions of an aqueous PF adhesive alone serve poorly as a binder or as a solvent to aid in penetration of higher molecular weight adhesive molecules (Stephens and Kutscha 1987). It is believed that the primary function of the low molecular weight adhesive is to cross-link between the higher molecular weight adhesive molecules. In addition, the low molecular weight PF adhesive fraction has been shown to have the greatest gross adhesive penetration into the wood substrate when wetting.

METHODS AND MATERIALS

Panel manufacturing

Three replicate steam injection flakeboard panels were manufactured for each adhesive. The panels were manufactured with *Liriodendron tulipifera* flakes cut with a 91-cm (36-in.) CAE disc flaker to target dimensions of 13 mm by 76 mm by 0.51 mm (0.5 in. by 3 in. by 0.020 in.). The flakeboard panels had dimensions of 610 mm by 610 mm by 25.4 mm (24 in. by 24 in. by 1 in.) with a specific gravity of 0.64. The mats were hand-felted with random orientation. Flake moisture content was approximately 3.4%, and mat moisture content going into the press was approximately 9.3%. The panels were pressed in a 300-ton, 610-mm by 610-mm (24-in. by 24-in.) Clifton hot press controlled by a programmable YEW process loop controller. Steam was supplied by a dedicated Coates 45 kW electric boiler. Platens were independently heated by a Sterlco Model F6026-D high temperature oil heater. The platens had 1.59-mm (0.0625-in.) diameter steam injection port holes spaced 57.2 mm (2.25 in.) apart. The outer 102 mm (4 in.) of the platens did not contain steam injection port holes.

A steam injection schedule similar to one used successfully with a liquid resole PF adhesive by Geimer et al. (1991) was used. Total press time was approximately 400 seconds, with 27 seconds of 1.37 MPa (200 psi) steam injected during press closing. Due to the finite steam supply, steam pressure declined throughout the steaming period. Steaming was initiated in a 15-sec hold stage in which press closing ceased when the mat reached a specific gravity of 0.27. Press closing was again started and steaming continued until approximately 5 seconds after the mat reached final platen position. A 25.4-mm wide by 6.35-mm thick (1-in. by ¼-in.) steel dam was inserted into the outer edge of the mat to help maintain internal gas pressure, mimicking a commercial scale press. Steel screens with dimensions of 610 mm by 610 mm by 1.78 mm (24 in. by 24 in. by 0.070 in.) were used on top and bottom of the mat to help distribute the steam more evenly. The outer 102 mm (4 in.) of the screens were sealed with a high temperature silicone RTV sealant to slow leakage of steam. The press platens were heated to 200 C. Press conditions as well as temperature in the mat were recorded through a computer-based data acquisition system. After steaming ceased, the solenoid steam valve system remained closed, and steam was allowed to dissipate from the press manifold through the mat for 82 sec. Afterwards, the steam control valve was opened, and the press manifold was allowed to vent to atmosphere for 10 sec. A pneumatic vacuum ejector was then employed through the press manifold for the rest of the pressing cycle to aid in removal of moisture from the mat.

Adhesive characterization

Three liquid resole phenol-formaldehyde adhesives were used to manufacture the panels. The adhesives used were identical, except for the degree of polymerization. The molecular weight distribution of the three adhesives was characterized by gel filtration chromatography (GFC) as performed by Sellers and

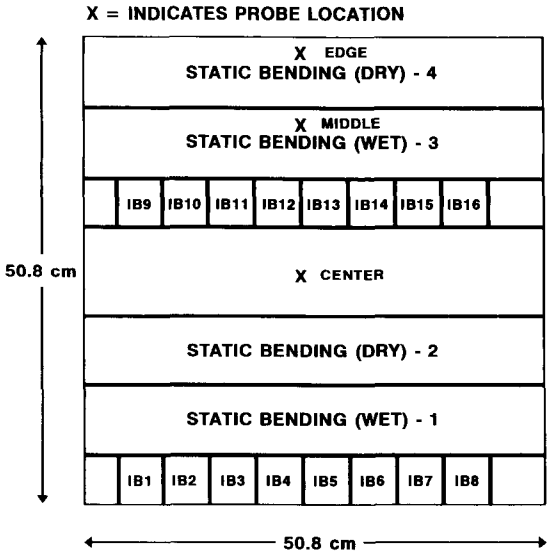

FIG. 1. Cutup diagram of flakeboard panels and location of thermocouple and gas pressure probes.

Prewitt (1990). The gel packing material was Sephacryl S-200, and an aqueous 0.1N NaOH eluent was used. Sodium polystyrene sulphonates and phenol were used as calibration standards. The UV detector was equipped with a 280-nm filter. Other pertinent adhesive physical properties such as viscosity, pH, and gel time were also measured. Resin solids were applied at 5% weight basis. No wax or sizing was added. The adhesive was applied to the flakes in a 45.7-cm by 122-cm (18-in. by 48-in.) rotating drum blender with a pneumatic atomizing nozzle. Air pressure to the nozzle was 152 kPa (25 psi) and the blender rotated at 0.27 rps (16 rpm).

Mechanical tests

Figure 1 shows the panel cutup diagram. Internal bond and static bending tests were performed according to ASTM D-1037-89 (1990). Sixteen internal bond specimens and four bending specimens were cut from each panel. Half of the internal bond specimens were cut from the edge of the panel (specimens 1–8) and half were cut from near the center of the panel (specimens 9–16). Two static bending specimens were tested dry (specimens 2 and 4), and two were tested wet (specimens 1 and 3). Both wet bending specimens were from similar locations in the panel, but dry bending samples 2 and 4 were cut from locations close to the board center and edge, respectively.

Quantifying adhesive penetration

Flakes of *Liriodendron tulipifera* were sliced from the same log that was used to produce the panel furnish. The flakes were sequentially sliced from the relatively permeable sapwood of a water-saturated block with the width orientation as close to the pure tangential plane as possible. The flakes were dried in a convection oven at 104 C to oven-dry condition. Target flake dimensions were 25.4 mm by 25.4 mm by 0.635 mm (1 in. by 1 in. by 0.025 in.). Five minutes after removal from the oven, three drops of liquid phenol-formaldehyde adhesive were placed across the width of each flake with a micropipette set at 0.50 microliters volume. The flakes and each adhesive drop were weighted on an analytical balance. The flakes had a 5-min open assembly time. Half of the flakes were placed in a convection oven heated to 104 C overnight. These flakes will later be referred to as unpressed flakes. The other flakes, which contained adhesive drops, were mated with an opposing flake that contained no adhesive and were placed in a teflon fabric envelope. The envelope was produced from Spectrum® fluorocarbon macro filter with 174-μm mesh opening, 180-μm thickness, and 24% open area. The envelope containing the flake assemblies was placed in a flakeboard mat, exposed to a steam injection pressing environment, and later recovered from the panel. These flakes will be referred to as pressed flakes in later discussion. The press and steaming schedule that was used to produce this panel was similar to the one used to produce the nine flakeboard panels.

Cross sections of the cured adhesive on flake specimens were cut 80 μm thick on a sliding microtome. These cross sections were stained with 0.5% Toluidine Blue O solution. After

staining, a fluorescence microscope interfaced with an image analysis system was then used to quantify adhesive penetration into the flakes. The staining and image analysis techniques have been described previously (Johnson and Kamke 1992). A Carl Zeiss Axioskop microscope with 50W mercury burner and halogen bulbs was used for observing the sections. The sections were viewed under incident light with a 10× Plan Neofluar objective providing a microscopic magnification of 80×. Total magnification on the image analysis system was 320×. An UV G365/LP420 excitor-barrier filter set was used. Measurements were performed with a (Universal Imaging) Image 1/AT Image Processing and Analysis System. The system consisted of a CCD solid-state camera, a 30 lines per millimeter 330 mm color monitor, a WIN 386 personal computer with monitor, a frame grabber board, and the Image 1/AT software. The staining technique used in this project suppresses the autofluorescence of the wood, while allowing the nonabsorbent adhesive to fluoresce brightly. Therefore, measurements conducted in this experiment are of adhesive area on the transverse plane, herein referred to as adhesive penetration area. The sections were positioned such that the left edge of the image consisted of the wood-adhesive interphase region, with the flake thickness in the radial direction lying across the long axis of the monitor screen. The target flake thickness was 635 μm, while the monitor screen corresponded to an area 623 μm high by 800 μm wide. Therefore, the flake thickness (in most cases) was less than 800 μm and lay completely within the image. Measurements of any adhesive that did not penetrate beneath the flake surface were also made. One-half of a bondline was analyzed in the pressed flake assemblies. Each image was analyzed as a whole, and then in individual segments 100 μm wide by the monitor screen height (623 μm). Up to 8 segments were analyzed for each image, starting at the wood-adhesive interface and analyzing 100-μm wide segments across the flake thickness.

TABLE 1. *Analysis of liquid resole phenol-formaldehyde physical properties and molecular weight parameters as measured by gel filtration chromatography.*

	Adhesive 1	Adhesive 2	Adhesive 3
pH	9.20	9.20	9.20
Nonvolatiles (%)	45.81	46.18	46.28
Viscosity (cP at 25 C)	82	138	200
Gel time (min)	23.50	20.90	19.96
NaOH (%)	1.45	1.45	1.45
Molecular weight averages			
Weight average (Mw)	2,964	3,680	4,366
Number average (Mn)	1,322	1,298	1,153
Z average (Mz)	6,159	7,713	10,440
Polydispersity (Mw/Mn)	2.241	2.835	3.786
	Area Adhesive 1	Area Adhesive 2	Area Adhesive 3
Molecular weight range			
73,500–35,000	0.00	0.00	0.11
35,000–18,000	0.40	1.14	2.95
18,000–10,000	3.89	6.50	8.94
10,000–5,000	12.70	15.50	16.47
5,000–3,000	15.06	16.33	13.89
3,000–2,000	15.27	15.63	14.63
2,000–1,000	25.95	24.17	21.13
1,000–500	20.29	16.22	15.58
500–100	6.44	3.46	7.73

RESULTS AND DISCUSSION

GFC results

GFC analysis results and other resin physical properties are listed in Table 1. The weight average molecular weight (Mw), and Z average molecular weight (Mz) increase from Adhesive 1 to Adhesive 3. These parameters, as well as the discrete molecular weight ranges, viscosity, and gel time, all indicate that Adhesive 3 is more highly developed than Adhesive 2, and Adhesive 2 is more highly developed than Adhesive 1. The number average molecular weight (Mn) decreases slightly from Adhesive 1 to Adhesive 3. This parameter is determined by the number of molecules in a molecular weight range, which is influenced by the large proportion of low molecular weight molecules found in all three adhesives. Polydispersity (Mw/Mn) increases from Adhesive 1 to Ad-

TABLE 2. *Mechanical properties of steam injection pressed flakeboard produced with 3 liquid resole phenol-formaldehyde adhesives.*

Adhesive	IB_{all} (kPa)	IB_{center} (kPa)	IB_{edge} (kPa)	Dry MOR_{all} (MPa)	Dry MOR_{center}	Dry MOR_{edge} (MPa)	Dry MOE_{all} (MPa)	Dry MOE_{center} (MPa)	Dry MOE_{edge} (MPa)	Wet MOR (MPa)	Wet MOE (MPa)	24 hour thickness swell (%)
Adhesive 1												
n	44	17	27	6	3	3	6	3	3	6	6	6
Mean	246	181	287	25.1	18.7	31.5	4,040	2,940	5,130	11.9	1,710	19.6
SD	113	78.4	113	11.0	2.02	13.1	1,610	1,080	1,320	1.85	245	3.44
Adhesive 2												
n	47	17	30	6	3	3	6	3	3	6	6	6
Mean	301	181	369	24.0	12.1	35.8	3,910	2,220	5,610	10.9	1,520	17.7
SD	160	84.2	153	16.7	2.88	16.5	2,060	438	1,330	1.67	120	2.52
Adhesive 3												
n	38	17	21	6	3	3	6	3	3	6	6	6
Mean	275	143	382	20.6	10.3	30.9	4,020	2,260	5,780	7.99	1,390	18.3
SD	159	99.1	109	13.7	2.77	12.0	2,310	627	1,910	2.19	190	4.19
F statistic	3.08	1.34	3.78*	0.230	5.91*	0.190	0.460	0.030	0.860	4.12*	2.50	1.24

F statistic is from GLM procedure with specimen density as covariant; * = significant at alpha = 0.05.

hesive 3. These adhesives were commercially produced and had molecular weight distribution parameters similar to those of a commercial flakeboard resin analyzed by Stephens and Kutscha (1987). A commercially prepared oriented strandboard resin analyzed by Sellers and Prewitt (1990) had substantially lower number and weight average molecular weights and greater polydispersity than any of the adhesives analyzed in this project.

Mechanical properties

a) Internal bond.—All three adhesives yielded poorly bonded panel surfaces. This probably resulted from a combination of convective heat (from steam) and conductive heat from the platens curing the adhesive on the mat surface before the mat reached final density. Therefore, internal bond specimens required sanding before they were tested. In Table 2, internal bond (IB) strengths and other mechanical properties of the panels are listed. The mean IB strength was low and variability was high for panels produced with all three adhesives. IB was not significantly different between the three board types. However, when IB specimens were grouped according to location relative to the edge of the pane (center or edge), differences could be attributed to the adhesives. Specimens 10–15 in Fig. 1 were labeled as the center IB group, and the remaining specimens were labeled as the edge IB group (1–9, and 16). For all three adhesives, edge IB strengths were higher than those from the panel center. There was no difference in center IB strengths between the three adhesives. However, Adhesives 2 and 3 had significantly higher edge IB strengths than Adhesive 1. ANOVA tests were also performed on other panel-related variables (Table 3). Location in the panel, between board variability, and IB specimen density all significantly affected IB strengths. The effect of specimen location and between board strength variability (within each group of 3 boards) increased with the higher weight average molecular weight adhesives. IB strength was highly correlated with specimen density, which in turn was highly correlated with specimen location in the panel. Therefore, all F statistics in Table 2 were calculated with the General Linear Model (GLM) procedure using specimen density as a covariant.

b) Bending specimens.—GLM analysis performed on modulus of rupture (MOR) and

modulus of elasticity (MOE) of dry bending samples showed no differences between the three adhesives (Table 2). One dry bending sample came from a location near the panel edge, and one came from the panel center. Edge MOR strengths and MOE stiffness were higher than those from samples located in the panel center. Adhesive 1 had significantly higher ultimate bending strength for the center samples than did Adhesive 2 or 3. No difference could be detected between adhesives for the panel edge bending MOR strengths. No difference could be detected between adhesives for dry bending MOE stiffness for edge or center specimens. As with the IB specimens, MOR strength and MOE stiffness was highly correlated with specimen density (Table 3).

Wet bending specimens 1 and 3 came from similar locations in the panel. MOR wet bending strengths for Adhesives 1 and 2 were significantly higher than those for Adhesive 3. There were no significant differences in 24-hour thickness swell between the 3 adhesives.

TABLE 3. *Effect of variables on some flakeboard properties as measured by* F *statistic from ANOVA analysis.*

Property	Adhesive	Location in panel	Specimen density	Between board variability
Internal bond				
IB_{all}	1.61	68.5*	102.0*	11.7*
IB_{center}	1.05	—	242.0*	3.92*
IB_{edge}	4.51*	—	574.0*	21.6*
$IB_{Adhesive\ 1}$	—	11.4*	29.7*	7.19*
$IB_{Adhesive\ 2}$	—	24.9*	20.8*	15.2*
$IB_{Adhesive\ 3}$	—	48.9*	91.6*	17.4*
Drying bending properties				
MOR_{all}	0.170	19.0*	115.0*	0.350
MOE_{all}	0.0100	34.0*	99.4*	0.250

* = Significant at alpha = 0.05.

Mat environment

In a preliminary panel, gas pressure and temperature were measured in three locations using a technique similar to that of Kamke and Casey (1988). The three locations are denoted in Fig. 1 as edge, middle, and center. The press and steam schedule was very similar to those used to produce the nine flakeboards. All measurements were taken in the mat core. Temperature and vapor pressure measurements were taken in the center of the mat (center), 15.2 cm (6 in.) in from the mat edge (middle), and 7.62 cm (3 in.) in from the mat edge (edge) as shown in Fig. 1. Temperatures and gas pressures increase as the distance from the edge of the mat increases, with the highest recorded measurements in the center (Fig. 2). Further investigation of the gas pressure measurements shows that when steam injection is initiated, there is an immediate temperature rise; but the pressure rise is more gradual, lagging behind the calculated saturated vapor pressure of liquid water. This indicates a low resistance to steam flow escaping through the edge of the mat and condensation, causing rapid heat transfer. Shortly after the steam supply is stopped, the environment achieves saturation and remains saturated throughout the remainder of the press cycle. Evaporative cooling causes a reduction in temperature as the internal gas pressure is allowed to dissipate. As seen in Fig. 3, liquid hydraulic pressure may have existed in the mat center after steam injection ceased as evidenced by a greater measured gas pressure than the saturated steam pressure at the prevailing temperature. At the

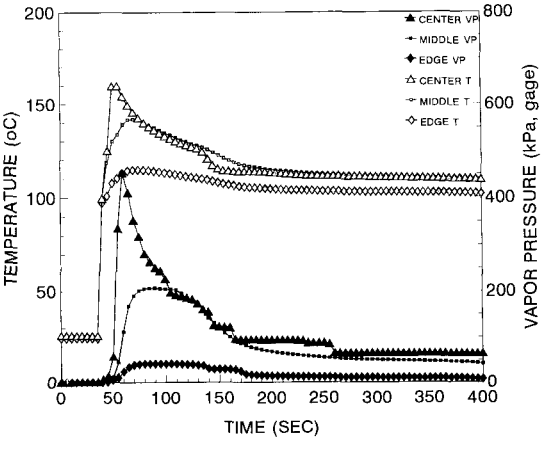

FIG. 2. Temperature and vapor pressure measured at 3 locations in the mat core during steam injection pressing.

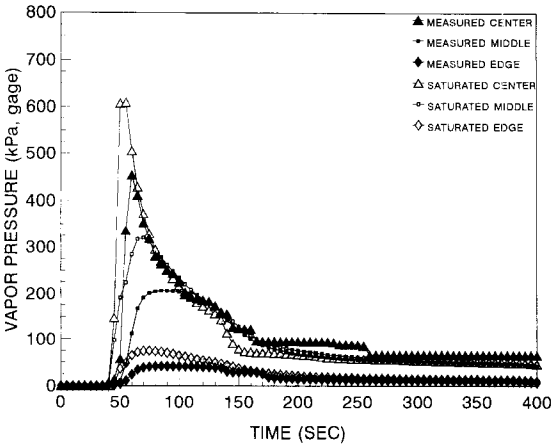

FIG. 3. Measured vapor pressure and calculated saturated vapor pressure at the measured temperature shown for 3 locations in the mat during steam injection pressing.

middle and edge positions, the measured gas pressure precisely follows the saturated vapor pressure line after venting is initiated at 130 seconds. Apparently the middle and edge positions receive a continuous supply of saturated water vapor from the center of the mat. Immediately following initiation of steam injection, superheated conditions appear to exist in all three locations. As the distance from the mat edge increased, the time at a superheated condition decreased. A period of low relative saturation at sufficient temperatures could be critical in accelerating PF adhesive cure kinetics and bond strength development. This could help explain the poor mechanical properties found in the center of the panels. Excessive condensation and liquid water formation are accentuated by poor quality steam and high mat moisture content.

Adhesive penetration

Table 4 summarizes the results of the adhesive penetration area measurements. For each adhesive, ten images were analyzed from a total of three adhesive drops for the unpressed flakes. Because of higher expected variability, a larger sample size of twenty images was analyzed from a total of six adhesive drops per adhesive for the pressed flakes. General trends can be observed using penetration

TABLE 4. *Image analysis measurements of adhesive penetration area in unpressed flakes and steam injection pressed flakes.*

Distance from flake surface (0–800 μm)	Adhesive 1		Adhesive 2		Adhesive 3		Mean	
	Unpressed	Pressed	Unpressed	Pressed	Unpressed	Pressed	Unpressed	Pressed
Adhesive penetration area (μm^2)								
0–100	18,000	10,900	27,500	11,500	27,100	8,940	24,210	10,450
100–200	24,400	11,200	11,500	11,000	6,980	10,800	14,290	11,000
200–300	20,600	9,540	200	7,310	1,190	5,800	7,350	7,550
300–400	6,010	6,440	0	3,760	0	1,960	2,000	4,050
400–500	860	1,840	0	1,430	0	50	290	1,430
500–600	0	2,260	0	300	0	0	0	870
600–700	10	340	0	110	0	0	0	150
700–800	0	100	0	0	0	0	0	30
Sum	69,880	42,620	39,200	35,410	35,270	27,550	48,140	35,530
Average size (μm^2) of adhesive objects								
0–100	500	200	1,260	250	810	160	860	210
100–200	1,490	350	2,420	470	2,540	450	2,150	420
200–300	2,250	720	776	390	1,660	490	1,562	530
300–400	755	680	0	270	0	410	250	450
400–500	675	270	0	160	0	280	225	240
500–600	0	370	0	60	0	50	0	160
600–700	10	110	0	70	0	0	0	60
700–800	0	110	0	0	0	0	0	40

data averaged for the three adhesives for comparison between pressed and unpressed flakes. The unpressed flakes contained a greater amount of adhesive penetration area than the pressed flakes in the first 200-μm distance from the flake surface. The pressed and unpressed flakes contained similar amounts of adhesive penetration area in the segment 200–300 μm from the flake surface. The pressed flakes contained a greater amount of adhesive penetration area than the unpressed flakes at 300–800-μm distance in from the flake surface. Adhesive objects are defined here as discrete adhesive penetration areas measured on the transverse plane of the flake. The pressed flakes had a larger number of adhesive objects tallied in all segments, whereas the average size for adhesive objects was greater in most segments for the unpressed flakes. Less total adhesive penetration area was present in the pressed flakes than in the unpressed flakes. The pressed flakes were mated with a flake with no adhesive, so some of the adhesive transferred to the other flake surface.

More of Adhesive 1 penetrated into the wood substrate than Adhesive 2 or 3 for both the pressed and unpressed flakes. Much of Adhesives 2 and 3 did not penetrate past the flake surface on the unpressed flakes (Johnson and Kamke 1992). Statistical analysis performed on these data detected significant differences in adhesive penetration area measurements between Adhesive 1 and the other two adhesives in the unpressed flakes for the segments within 300 μm of the flake surface. However, significant differences in penetration between the three adhesives are much less apparent in the pressed flakes. There was greater adhesive penetration area with Adhesive 1 than Adhesive 3 in the segments from 200–400 μm from the flake surface. Adhesive 1 had significantly greater adhesive penetration area than Adhesive 2 or 3, and Adhesive 2 had greater adhesive penetration area than Adhesive 3 in the segment 500–600 μm in from the flake surface. Observations made by the authors indicated that very little adhesive was left at the bondline on the pressed flakes. Figures 4a and 4b show examples of unpressed and pressed flakes for Adhesive 2, respectively. When the flake assemblies were produced, adhesive that did not penetrate during wetting of the flake surface was likely compressed along the flake surface and into vessel elements inclined towards the flake surface. Further movement of the adhesive likely occurred during exposure to the steam injection environment as the viscosity would decline due to an increase of temperature and further dilution of the adhesive. For yellow poplar, vessel elements proved to be the dominant avenue of flow for adhesive in the unpressed flakes (Johnson and Kamke 1992). As seen in Fig. 4b, it appears that vessels also play a dominant role in the pressed flakes.

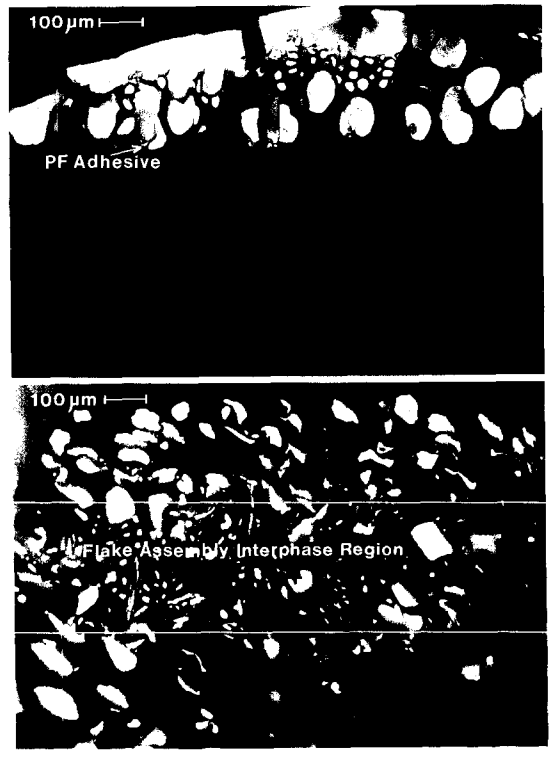

FIG. 4a. Photomicrograph of adhesive interphase region on unpressed *Liriodendron tulipifera* flake surface (Adhesive 2).

FIG. 4b. Photomicrograph of adhesive interphase region in steam injection pressed *Liriodendron tulipifera* flake assembly (Adhesive 2).

In both pressed and unpressed flakes, many fiber lumens are filled with adhesive near the flake surface; but as distance from the flake surface increases, the vessel elements contain a greater proportion of adhesive penetration area. For both the pressed and unpressed flakes, the average adhesive object size increases as the distance from the flake surface increases, reaches a maximum, and then decreases. The maximum average area is in the segment where the highest concentration of fully filled vessel lumens exists. Statistical analysis performed on the average size of adhesive objects detected few significant differences between the adhesives in the unpressed and pressed flakes. The large difference in lumen size between vessels and fibers and the small area over which measurements were tallied relative to vessel lumen size added to the difficulty in determining significant differences in the average size of adhesive objects that could be related to the adhesive.

CONCLUSIONS

In this research project, mechanical properties of panels produced with steam injection pressing were significantly lower in the center of the panel than at the edge of the panel. The mat environment at the edge of the panel has a lower relative saturation and less potential for liquid water condensate. Poor quality steam and high mat moisture content may have caused excess steam condensation in the center of the mat. These conditions were not favorable for bond strength development and may have masked the effect of adhesive molecular weight distribution. The effect of molecular weight distribution of the liquid resol PF on panel mechanical properties was not obvious. The two higher weight average molecular weight liquid resole PF adhesives produced greater IB strengths at the panel edge than the less developed adhesive.

The flow of adhesive into the wood ultrastructure was deeper and less concentrated in flakes exposed to a steam injection environment than in flakes wetted with adhesive and then placed in a convection oven. Flow of adhesive into the wood flakes that were not exposed to a pressing environment was considerably deeper with the lower weight average molecular weight adhesive than with the higher weight average molecular weight adhesives. There was less difference in depth and area of penetration between the three adhesives when exposed to the steam injection pressing environment in the center of the mat. This suggests that the range of the molecular weight distribution studied here may not have been great enough with the wet curing environment in the center of the mat to ascertain differences in mechanical properties and adhesive flow. Recommendations for future work in this area would be: (1) promote a dryer mat environment during steam injection, (2) use a wider range of adhesive molecular weight distributions, or (3) use molecular weight fractionation methods to separate adhesive into more discrete molecular weight components and independently analyze their performance (Stephens and Kutscha 1987; Wilson et al. 1979). A drier mat environment could be promoted by low moisture content furnish, high quality steam, shorter steam times, and lower steam pressure.

ACKNOWLEDGMENTS

The authors would like to thank Neste Resins Corporation for donation of materials and the Mississippi Forest Products Utilization Laboratory at Mississippi State University for providing GFC analysis. This project was performed in part by Jeff Brule as an undergraduate research project supported by the Center for Adhesive and Sealant Science at Virginia Tech.

REFERENCES

AMERICAN SOCIETY FOR TESTING MATERIALS. 1990. Standard test methods of evaluating the properties of wood-base fiber and particle panel materials. ASTM D-1037-89. Annual book of ASTM standards, vol. 04.09. Philadelphia, PA.

GEIMER, R. L., AND A. W. CHRISTIANSEN. 1991. Adhesive curing and bonding: Response to real time conditions. *In* Proceedings of the Adhesives and Bonded Wood Products Symposium, Nov. 19–21, 1991, Seattle, WA.

———, S. E. JOHNSON, AND F. A. KAMKE. 1991. Response of flakeboard properties to changes in steam injection environments. Res. Paper FPL-RP-507. USDA Forest Service, Forest Products Lab., Madison, WI.

GOLLOB, L., R. L. KRAHMER, J. D. WELLONS, AND A. W. CHRISTIANSEN. 1985. Relationship between chemical characteristics of phenol-formaldehyde resins and adhesive performance. Forest Prod. J. 35(3):42–48.

HATA, T., B. SUBIYANTO, S. KAWAI, AND H. SASAKI. 1989. Production of particleboard with steam injection press IV. Shortening the press cycle with steam injection. Mokuzai Gakkaishi 35(12):1087–1091.

JOHNSON, S. E., AND F. A. KAMKE. 1992. Quantitative analysis of gross adhesive penetration in wood using fluorescence microscopy. J. Adhesion 40:47–61.

KAMKE, F. A., AND L. J. CASEY. 1988. Fundamentals of flakeboard manufacture: Internal mat conditions. Forest Prod. J. 38(6):38–44.

NEARN, W. T. 1974. Application of the ultrastructure concept in industrial wood products research. Wood Sci. 6(3):285–293.

SELLERS, JR., T., AND M. L. PREWITT. 1990. Applications of gel filtration chromatography for resole phenolic resins using aqueous sodium hydroxide as solvent. J. Chromatography 513:271–278.

STEPHENS, R. S., AND N. P. KUTSCHA. 1987. Effect of resin molecular weight on bonding flakeboard. Wood Fiber Sci. 19(4):353–361.

SUBIYANTO, B., S. KAWAI, M. TANAHASHI, AND H. SASAKI. 1989. Curing conditions of particleboard adhesives II. Curing of adhesives under high steam pressures and temperatures. Mokuzai Gakkaishi 35(5):419–423.

WILSON, J. B., G. L. JAY, AND R. L. KRAHMER. 1979. Using resin properties to predict bond strength of oak particleboard. Adhesives Age, June 1979:26–30.